SUPPLEMENTAL MATERIAL

Supplemental Methods

Primary cultures of neonatal rat ventricular cardiomyocytes and reagents

Primary cultures of ventricular cardiomyocytes were prepared from 1-day-old Crl: (WI) BR Wistar rats (Charles River Laboratories). A cardiomyocyte-rich fraction was obtained by centrifugation through a discontinuous Percoll gradient. Cells were cultured in a complete medium (cardiomyocyte) containing Dulbecco's modified Eagle's medium (DMEM)/F-12 supplemented with 5% horse serum, 4 μg/ml transferrin, 0.7 ng/ml sodium selenite (Life Technologies, Inc.), 2 g/liter bovine serum albumin (fraction V), 3 mM pyruvic acid, 15 mM HEPES, 100 μM ascorbic acid, 100 μg/ml ampicillin, 5 μg/ml linoleic acid and 100 μM 5-bromo-2'-deoxyuridine (Sigma). Trehalose and rapamycin were purchased from Sigma.

Generation of Tg-Rheb mice

A tetracycline-responsive binary α-MHC transgene system was used to allow temporally regulated expression of wild-type Rheb in cardiomyocytes [1]. Mice were generated on a FVB background. Doxycycline was administered in the food with a special diet formulated by Purina (625 mg/kg in pellets). In the experiments that required Rheb protein induction, doxycycline was removed from the food at 3-4 weeks of life, resulting in induced expression of Rheb a few weeks later. All experimental procedures with animals were approved by the Institutional Animal Care and Use Committee of the University of Medicine and Dentistry of New Jersey.

Construction of adenoviruses

Recombinant adenovirus vectors were constructed as described [2]. pBHGloxΔE1,3Cre (Microbix), including the ΔE1 adenoviral genome, was co-transfected with the pDC shuttle vector containing the gene of interest into 293 cells. We made replication-defective human adenovirus type 5 (devoid of E1) harboring full length wild-type Rheb cDNA (Ad-Rheb) and full length wild-type Atg7 (Ad-Atg7), and

we used adenovirus harboring beta-galactosidase (Ad-LacZ) as a control. For the construction of short hairpin RNA (sh-RNA) adenoviral expression vectors, p*Silencer* 1.0-U6 expression vector was purchased from Ambion. The U6 RNA polymerase III promoter and the polylinker region were subcloned into the adenoviral shuttle vector pDC311 (Microbix). The hairpin-forming oligos of Rheb, Beclin-1, Raptor, Rictor and TSC2 rat cDNA and their antisenses with ApaI and Hind III overhangs were synthesized, annealed and subcloned distal to the U6 promoter. Recombinant adenoviruses were generated using homologous recombination in 293 cells. Cardiomyocytes were transduced with adenovirus for 48 hours in case of overexpression, and for 96 hours for sh-RNA-mediated knock-down.

Echocardiography

Echocardiography was performed after mice were anesthetized with 12 µl/g body weight of 2.5% Avertin, as described previously [2].

Prolonged ischemia

Pathogen-free mice were housed in a temperature-controlled environment with 12 hr light/dark cycles, where they received food and water ad libitum. Mice were anesthetized by intraperitoneal injection of pentobarbital sodium (60 mg/kg). A rodent ventilator (model 683;
Harvard Apparatus Inc) was used with 65% oxygen during the surgical procedure. The animals were kept warm using heat lamps and heating pads. Rectal temperature was monitored and maintained between 36.5 and 37.5°C. The chest was opened by a horizontal incision through the muscle between the ribs (third intercostal space). Ischemia was achieved by ligating the anterior descending branch of the left coronary artery (LAD) using an 8-0 nylon suture, with a silicon tubing (1 mm OD) placed on top of the LAD, 2 mm below the border between left atrium and left ventricle (LV). Regional ischemia was confirmed by ECG change (ST elevation).

Assessment of area at risk and infarct size

After 3 hours of ischemia, the animals were reanesthetized and intubated, and the chest was opened. After arresting the heart at the diastolic phase by KCl injection, the ascending aorta was cannulated and perfused with saline to wash out blood. To demarcate the ischemic area at risk (AAR), Alcian blue dye (1%) was perfused into the aorta and coronary arteries. Hearts were excised, and LVs were sliced into 1-mm thick cross sections. The heart sections were then incubated with a 1% triphenyltetrazolium chloride (TTC) solution at 37°C for 10 min. The infarct area (pale), the AAR (not blue), and the total LV area from both sides of each section were measured using ImageJ (NIH) and Adobe Photoshop (Adobe Systems Inc.), and the values obtained were averaged. The percentages of area of infarction and AAR of each section were multiplied by the weight of the section and then totaled from all sections. AAR/LV and infarct area/AAR were expressed as percentages. The extent of necrosis after 30 minutes of ischemia was quantified through Hairpin-2 staining (See below), since TTC staining is less accurate for the assessment of infarct size after this period of time[3].

High fat diet (HFD) mice feeding

C57BL/6J wild-type mice, heterozygous *Beclin-1* systemic knock-out mice, conditional *mTOR* knock-out mice crossed with α-MHC-*MerCreMer* mice (C57BL/J background), and heterozygous GFP-LC3 transgenic mice (C57BL/6J background, strain GFP-LC3#53, RIKEN BioResource Center) containing a rat LC3-GFP fusion under control of the chicken ß-actin promoter, were fed ad libitum with HFD (Research Diets D12492) for 18-20 weeks. A control group of mice matched for age and gender was fed with control diet for the same period of time.

Mice hematochemical analysis

Serum levels of glucose, cholesterol, triglycerides and non-esterified fatty acids (NEFA) in mice fed with control diet and high-fat diet were assessed by *in vitro* enzymatic colorimetric methods (Wako), according to the manufacturer's instructions. Serum levels of insulin were assessed with an ELISA assay (Crystalchem).

Evaluation of apoptosis in tissue sections

DNA fragmentation was detected *in situ* using the TUNEL assay, as described previously [2]. Briefly, deparaffinized sections were incubated with proteinase K, and DNA fragments were labeled with fluorescein-conjugated dUTP using TdT (Roche Molecular Biochemicals). Nuclear density was determined by manual counting of DAPI-stained nuclei in six fields for each animal using the 40x objective, and the number of TUNEL-positive nuclei was counted by examining the entire section using the same power objective.

TUNEL staining in cultured cardiomyocytes

Myocytes were fixed in PBS containing 4% paraformaldehyde. Staining was performed using the In Situ Cell Death Detection kit (Roche).

Assessment of necrosis *in vivo* with Hairpin-2 staining

A double-stranded DNA fragment with blunt ends was prepared as previously described [4, 5]. Polymerase chain reaction (PCR) with Pfu Ultra polymerase was performed with 16.6 μM Texas Red-12-dUTP (Molecular Probes), 16.6 μM dTTP, 50 μM dATP, 50 μM dCTP and 50 μM dGTP. The Pfu probe recognizes a form of DNA damage characterized by cleavage of multiple DNA fragments with blunt ends, typically observed in necrotic cell death [6]. Heart sections were deparaffinized with xylene, rehydrated in graded alcohol concentrations, briefly washed in water and then treated with proteinase K (50 μg/ml) in PBS for 45 minutes at 37°C. After washing with PBS, a mix of 50 mM Tris-HCl, pH 7.8, 10 mM MgCl2, 10 mM, DTT, 1 mM ATP, 25 μg/ml BSA, 15% polyethylene glycol (8,000 mol wt, Sigma), 1 μg/ml Texas red-labeled DNA fragment and 250 U/ml DNA T4 ligase (Roche) was added. Sections were then placed in a humidified box for 16 hours. The sections were thoroughly washed in 70°C water and observed under a fluorescent microscope immediately after counterstaining with 10 μg/ml 4,6-diamidino-2-phenylindole (DAPI).

Cell size evaluation and histological analysis

Heart specimens were fixed with 10 % neutral buffered formalin, embedded in paraffin, and sectioned at 6-μm thickness. Cell size was assessed through wheat germ agglutinin staining, as previously described [2]. Immunofluorescent staining was performed with reagents and protocols previously described [7]. Cardiac myocytes were stained with anti-troponin T antibody. Alexa 488- and Alexa 594-conjugated secondary antibodies (Invitrogen) were used. Nuclei were stained with DAPI.

Viability of the cells

Viability of the cells was measured by Cell Titer Blue (CTB) assays (Promega). In sum, cardiomyocytes ($1x10^5$ per 100 μl) were seeded onto 96-well dishes. After 24 hours, the medium was changed to a serum free medium. Cardiomyocytes were transduced with adenovirus harboring Rheb, Atg7 or LacZ for 36-48 hours, or shRNA against Rheb, TSC2, Beclin-1 or scramble shRNA for 96 hours, and then changed to a glucose free medium for the time required by the experiment. Viable cell numbers were measured by the CTB assay. The CTB assays were performed according to the supplier's protocol. In vitro, necrosis was assessed through propidium iodide staining as previously described [4]

Evaluation of autophagy

Autophagy was assessed by three different methods: LC3-II accumulation, p62 accumulation and autophagosome formation [8, 9]. *In vivo*, LC3-II accumulation was evaluated in the early phase of ischemia (30 minutes), since LC3-II may be degraded and may not be reliable in the later phase [9]. Autophagy in the later phase of ischemia was assessed by accumulation of p62, a protein known to be degraded by autophagy [9], since p62 accumulation represents a more stable marker of autophagy. Autophagosome formation *in vivo* was evaluated by counting GFP-LC3 dots in at least seven independent fields of heart sections from Tg-GFP-LC3 mice. These mice selectively express LC3

conjugated to a green fluorescent protein in the heart [8]. GFP-LC3 dots were also evaluated after chloroquine administration (10 mg/kg i.p.) to evaluate autophagic flux, as previously described [10]. For analysis of autophagosome formation *in vitro*, cardiomyocytes were grown on gelatinized coverslips. Myocytes were transduced with Ad-GFP-LC3, viruses that express GFP-LC3, for 48 hours. Samples were mounted using a SlowFade Light Antifade Kit (MolecularProbes), and the fluorescence of GFP-LC3 was observed under a fluorescence microscope. The number of cells with GFP-LC3 dots was counted in at least seven independent visual fields.

Gene expression analysis

mRNA expression of p62, atrial natriuretic factor (ANF) and GAPH (loading control) was evaluated with quantitative real time PCR, as described[4]. The following primers were used: p62 sense 5'-CAGGCGCACTACCGCGATGA-3', antisense 5'-TCGCACACGCTGCACAGGTC-3'; ANF sense 5'-ATGGGCTCCTTCTCCATCAC-3', antisense 5'-ATCTTCGGTACCGGAAGCTG-3'; and GAPDH sense 5'-TTCTTGTGCAGTGCCAGCCTCGTC-3', antisense 5'-TAGGAACACGGAAGGCCATGCCAG-3';

Immunoblot analysis, antibodies and reagents

For immunoblot analyses, heart homogenates and cardiomyocyte lysates were prepared in a RIPA lysis buffer containing 50 mM Tris·HCl (pH 7.5), 150 mM NaCl, 1% Triton X-100, 0.1% SDS, 0.5% deoxycholic acid, 1 mM EDTA, 0.1 mM Na_3VO_4, 1 mM NaF, 50 μM phenylmethylsulfonyl fluoride (PMSF), 5 μg/ml aprotinin and 5 μg/ml leupeptin. The antibodies used include anti-Rheb (Cell Signaling Technology and Santa Cruz), phospho-p70S6K (Thr389, Cell Signaling Technology), p70S6K (Santa Cruz), phospho-4E-BP1 (Thr37/46, Cell Signaling Technology), 4E-BP1 and mTOR (Cell Signaling Technology), TSC2 (Santa Cruz), p62 (American Research Products, Inc.), LC3 (MBL), Bip (Cell Signaling Technology), phospho-PERK (Thr980, Cell Signaling Technology), CHOP (Santa Cruz), Caspase-12 and cleaved Caspase-3 (Cell

Signaling Technology), Beclin-1 (Pharmingen), Atg4 (MBL), Atg5 (MBL), Atg7 (MBL), Ulk1 (Abcam), phospho-IR (Tyr11262/3, Santacruz), phospho-IRS1 (Tyr989, Ser636, Santacruz), IR and IRS-1 (Cell Signaling Technology), phospho-Akt1 (Ser473, Millipore), Akt1 (Cell Signaling Technology), GAPDH (Sigma) and tubulin (Sigma).

Measurement of Rheb activity

Endogenous Rheb activity is commonly evaluated by the ratio of GTP and GDP bound to Rheb, as Rheb is highly active when it is rich in GTP [11]. Rheb-bound GTP and GDP amounts were assessed according to a previously described luminometric method [12, 13]. This method represents a well-established assay for the measurement of the activity of GTP-binding proteins [14, 15].

Proteins were extracted from cultured cardiomyocytes or mouse heart specimens in an ice-cold HEPES-based buffer containing 10 mM $MgCl_2$, protease inhibitors and 1% Igepal CA-630 [15]. The anti-Rheb C antibody or control IgG was added to the samples, which were shaken at 4°C overnight in the presence of 500 mM NaCl, 0.5% deoxycholate and 0.05% SDS. Protein G-agarose was then added to each sample. After shaking for 2 hours at 4°C, the agarose beads were washed four times in lysis buffer containing NaCl and detergents, and two times in 20 mM TrisPO_4, 5 mM $Mg2SO_4$. The beads were resuspended in 20 mM TrisPO_4, 1mM DTT, 1 mM EDTA, and heated at 100°C for 3 min to elute GTP and GDP bound to the immunoprecipitated Rheb. In each sample, GTP and the sum of GTP plus GDP were measured in coupled enzymatic assays [15]. GTP was converted to ATP by nucleoside diphosphate kinase (3 mu) in the presence of ADP (10 pmol), and the resulting ATP was measured by the luciferase method (4 mmol of luciferin and $8x10^8$ light units of luciferase). The sum of GTP plus GDP was measured by converting GDP to GTP using pyruvate kinase (3 mu) and phosphoenolpyruvate (50 μM). GTP, which at this point represents the sum of GDP plus GTP, was measured as described above. The GTP/GTP+GDP ratio was then calculated by the ratio of the emitted light in the two reactions.

Measurement of intracellular ATP content

Intracellular ATP content was measured using an ATP Bioluminescent Assay Kit (Sigma). Cells were scraped with PBS, and then half of them were used for protein content assay and the other half for ATP content measurement. For the latter assay, cells were lysed in the somatic-cell ATP-releasing agent, and the lysates were assayed according to the manufacturer's instructions, using a 1:625 dilution of the ATP assay mix. Light emitted was measured using a luminometer and was then normalized for protein content of the sample. For ATP content assays in myocardial tissue, heart specimens of equal weights were directly lysed in the somatic-cell ATP-releasing agent, and the lysates were assayed as described above.

Supplemental Tables

Table I. Echocardiographic parameters of Tg-Rheb.

	Parameters	NTg (N=4)	Tg-Rheb (N=4)
Echocardiographic parameters	SWTd (mm)	0.91 ± 0.05	0.94 ± 0.03
	LVEDD (mm)	3.89 ± 0.10	3.92 ± 0.11
	PWTd (mm)	0.87 ± 0.05	0.89 ± 0.03
	SWTs (mm)	1.48 ± 0.11	1.51 ± 0.09
	LVESD (mm)	2.31 ± 0.11	2.29 ± 0.05
	PWTs (mm)	1.21 ± 0.05	1.30 ± 0.08
	FS (%)	40.49 ± 1.23	41.38 ± 1.05

SWTd: diastolic septum wall thickness; LVEDD: left ventricular end-diastolic diameter; PWTd: diastolic posterior wall thickness. Data is presented as (mean ± SEM).

Table II. Body weight and hematochemical tests in HFD mice as compared with CD mice.

Parameters	Control diet (N=15)	High fat diet (N=15)
Body weight (g)	26.8 ± 1.0	54.6 ± 3.3*
Glucose (mg/dl)	112.9 ± 6.2	176.0 ± 17.3*
Insulin (ng/ml)	0.23 ± 0.01	0.43 ± 0.02*
HOMA Index	1.8 ± 0.22	5.8 ± 0.65*
Total cholesterol (mg/dl)	84.1 ± 3.1	126.1 ± 8.0*
Trygliceride (mg/dl)	36.3 ± 3.7	71.2 ± 9.5*
NEFA (meq/l)	0.93 ± 0.12	1.87 ± 0.35*

HOMA: Homeostatic Model Assessment; NEFA: not-esterified fatty acids. Data is presented as (mean ± SEM); *$p<0.05$.

Table III. Echocardiographic parameters of HFD mice.

	Parameters	CD (N=5)	HFD (N=6)
Gravimetric parameters	**HW/TL (mg/mm)**	6.4 ± 0.3	8.2 ± 0.4*
	LVW/TL (mg/mm)	4.1 ± 0.1	5.9 ± 0.4*
	RVW/TL (mg/mm)	0.9 ± 0.03	1.3 ± 0.07*
	Lung/TL (mg/mm)	7.9 ± 0.15	7.4 ± 0.28
Echocardiographic parameters	**SWTd (mm)**	0.88 ± 0.03	1.08 ± 0.05*
	LVEDD (mm)	3.85 ± 0.08	4.12 ± 0.08
	PWTd (mm)	0.85 ± 0.05	1.00 ± 0.03*
	SWTs (mm)	1.31 ± 0.04	1.51 ± 0.05*
	LVESD (mm)	2.30 ± 0.06	2.55 ± 0.05
	PWTs (mm)	1.26 ± 0.04	1.47 ± 0.06*
	FS (%)	39.26 ± 1.04	38.61 ± 0.99

Control diet: CD; HFD: high fat diet; HW: heart weight; LVW: left ventricular weight; RVW: right ventricular weight; TL: tibia length; SWTd: diastolic septum wall thickness; LVEDD: left ventricular end-diastolic diameter; PWTd: diastolic posterior wall thickness. Data is presented as (mean ± SEM); *$p<0.05$.

Fig. I

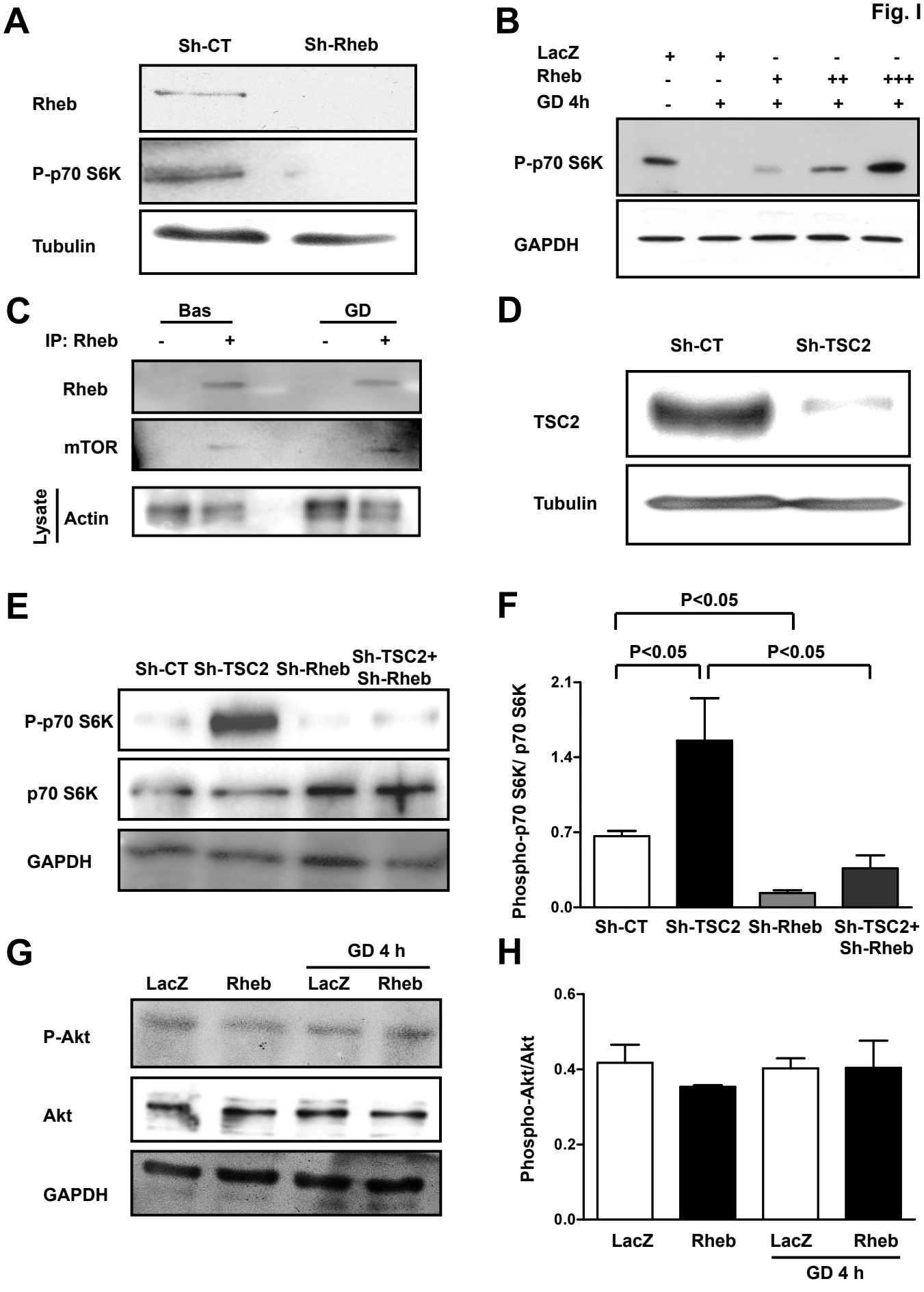
A
Sh-CT
Sh-Rheb
Rheb
P-p70 S6K
Tubulin
B
LacZ + + - - -
Rheb - - + ++ +++
GD 4h - + + + +
P-p70 S6K
GAPDH
C
Bas
GD
IP: Rheb - + - +
Rheb
mTOR
Lysate
Actin
D
Sh-CT
Sh-TSC2
TSC2
Tubulin
E
Sh-CT Sh-TSC2 Sh-Rheb Sh-TSC2+ Sh-Rheb
P-p70 S6K
p70 S6K
GAPDH
F
P<0.05
P<0.05
P<0.05
Phospho-p70 S6K/ p70 S6K
2.1
1.4
0.7
0.0
Sh-CT
Sh-TSC2
Sh-Rheb
Sh-TSC2+ Sh-Rheb
G
GD 4 h
LacZ
Rheb
LacZ
Rheb
P-Akt
Akt
GAPDH
H
Phospho-Akt/Akt
0.6
0.4
0.2
0.0
LacZ
Rheb
LacZ
Rheb
GD 4 h

Fig. II

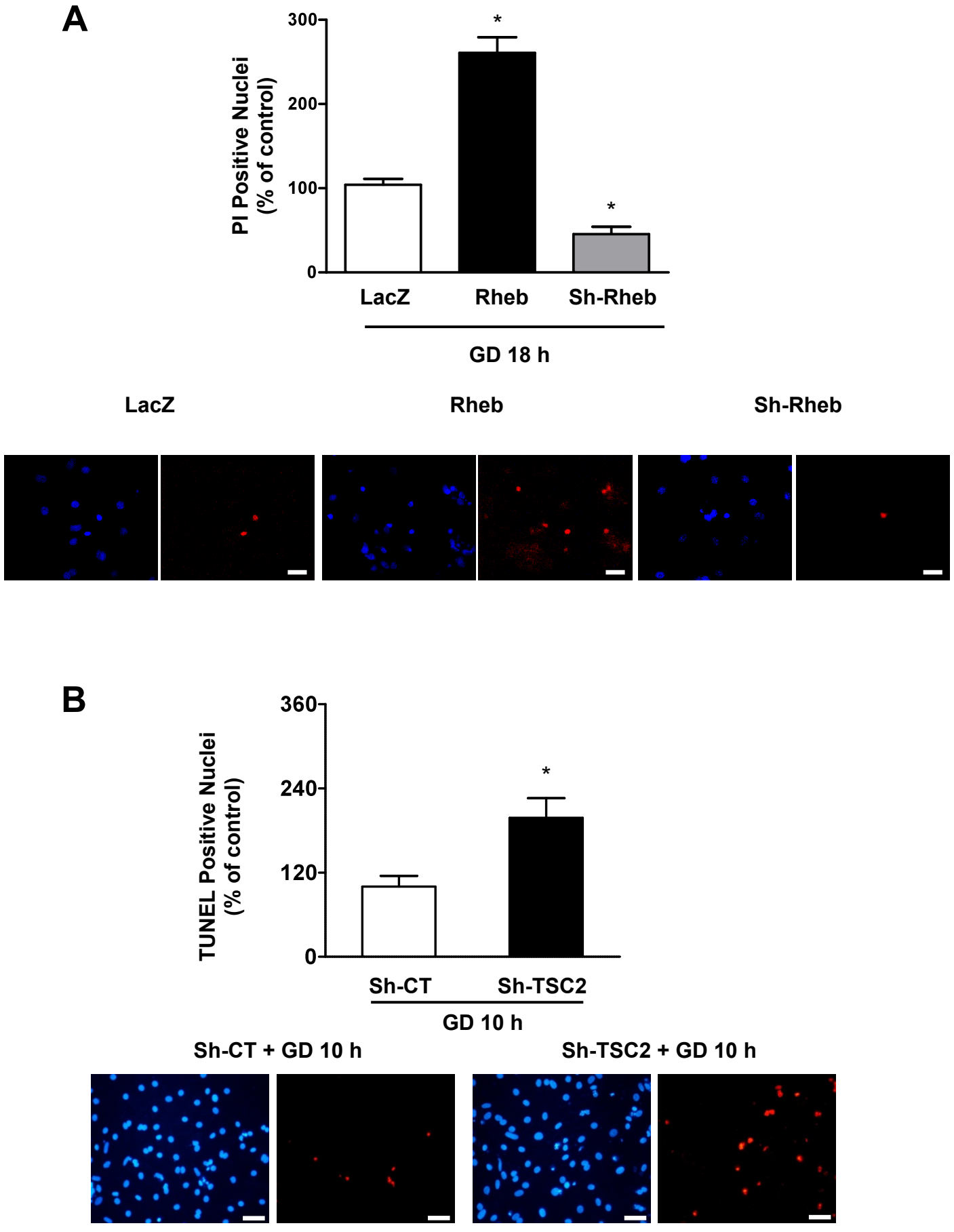
A
PI Positive Nuclei
(% of control)
300
200
100
0
*
*
LacZ
Rheb
Sh-Rheb
GD 18 h
LacZ
Rheb
Sh-Rheb
B
TUNEL Positive Nuclei
(% of control)
360
240
120
0
*
Sh-CT
Sh-TSC2
GD 10 h
Sh-CT + GD 10 h
Sh-TSC2 + GD 10 h

Fig. III

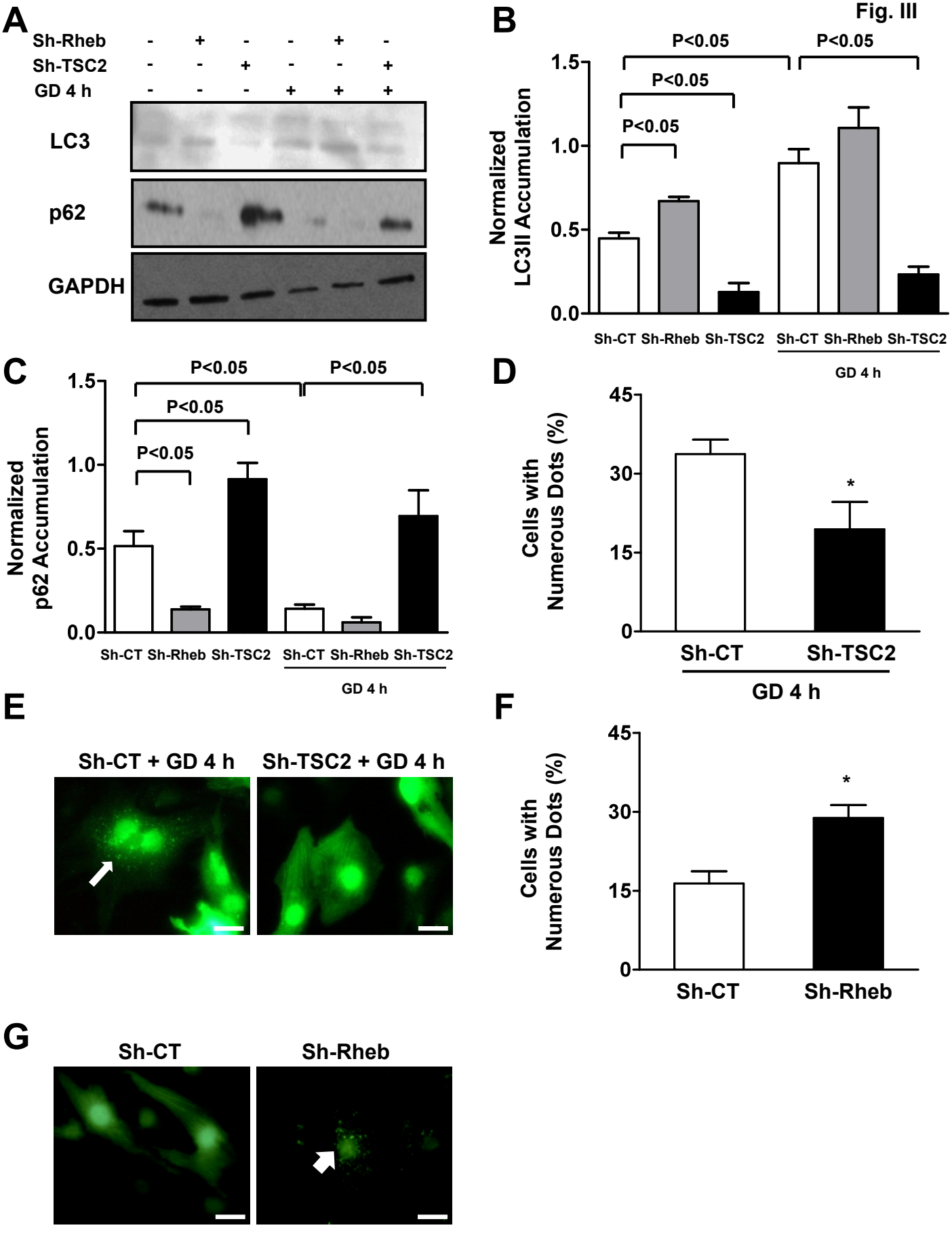
A
Sh-Rheb - + - - + -
Sh-TSC2 - - + - - +
GD 4 h - - - + + +
LC3
p62
GAPDH
B
Normalized LC3II Accumulation
P<0.05
P<0.05
P<0.05
P<0.05
1.5
1.0
0.5
0.0
Sh-CT Sh-Rheb Sh-TSC2 Sh-CT Sh-Rheb Sh-TSC2
GD 4 h
C
Normalized p62 Accumulation
P<0.05
P<0.05
P<0.05
P<0.05
1.5
1.0
0.5
0.0
Sh-CT Sh-Rheb Sh-TSC2 Sh-CT Sh-Rheb Sh-TSC2
GD 4 h
D
Cells with Numerous Dots (%)
45
30
15
0
*
Sh-CT
Sh-TSC2
GD 4 h
E
Sh-CT + GD 4 h
Sh-TSC2 + GD 4 h
F
Cells with Numerous Dots (%)
45
30
15
0
*
Sh-CT
Sh-Rheb
G
Sh-CT
Sh-Rheb

Fig. IV

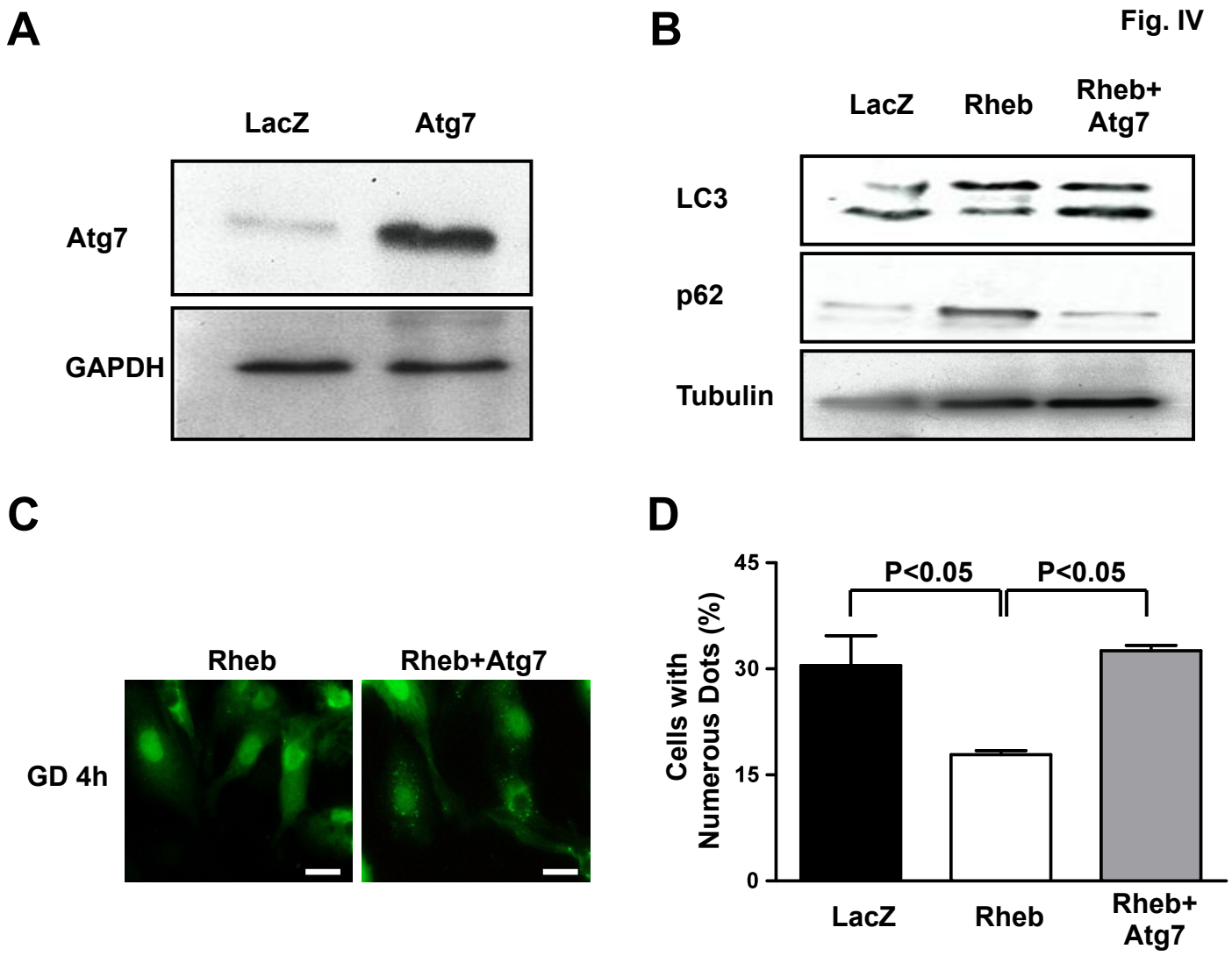
A
LacZ
Atg7
Atg7
GAPDH
B
LacZ
Rheb
Rheb+ Atg7
LC3
p62
Tubulin
C
Rheb
Rheb+Atg7
GD 4h
D
P<0.05
P<0.05
Cells with Numerous Dots (%)
45
30
15
0
LacZ
Rheb
Rheb+ Atg7
E
Trehalose 100 mM
- + - +
LacZ LacZ Rheb Rheb
LC3
p62
P-p70 S6K
GAPDH
F
Trehalose 100 mM
- - +
LacZ Rheb Rheb
Atg7
Beclin-1
GAPDH

Fig. V

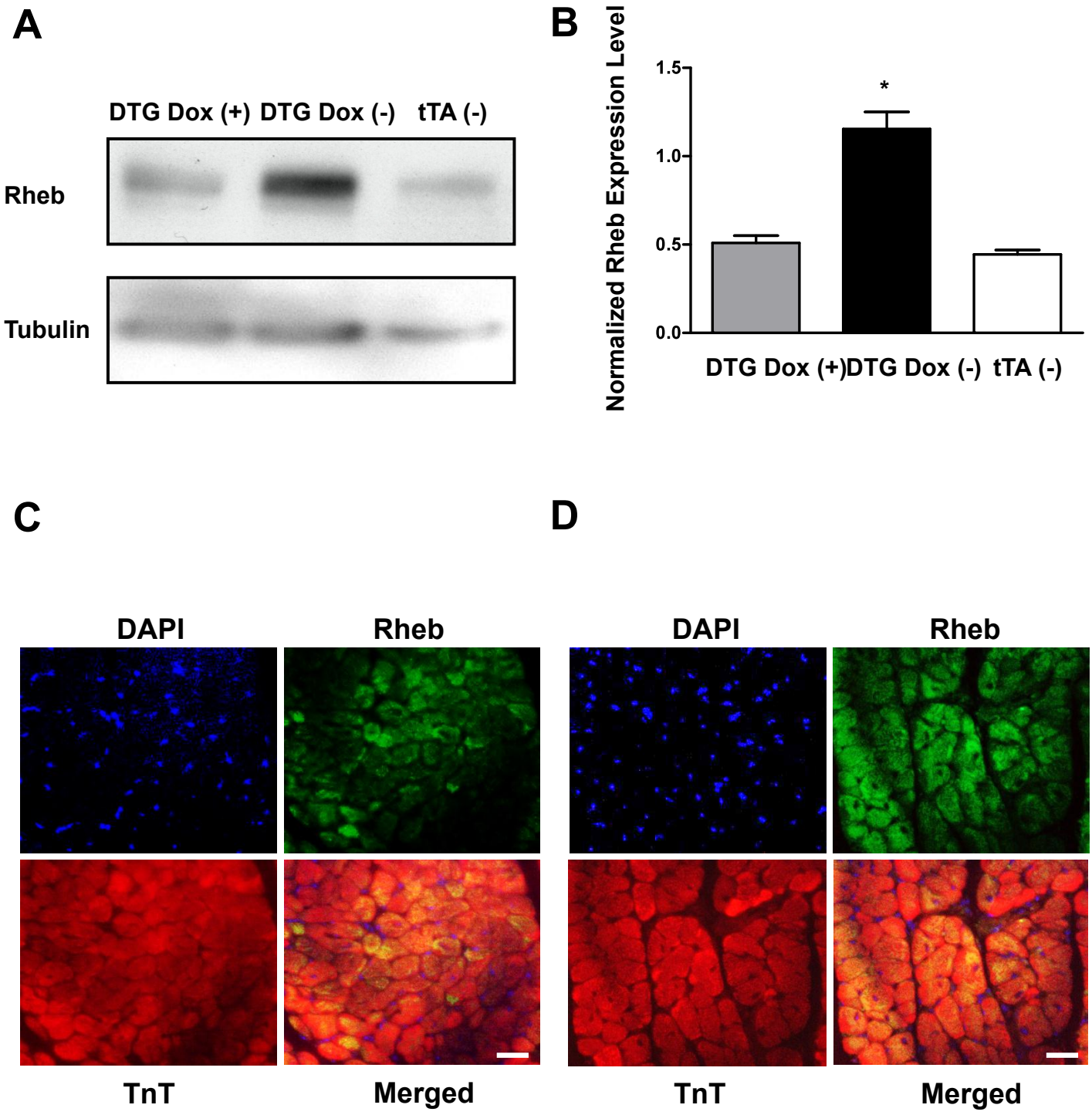
A
DTG Dox (+)
DTG Dox (-)
tTA (-)
Rheb
Tubulin
B
Normalized Rheb Expression Level
1.5
1.0
0.5
0.0
*
DTG Dox (+)
DTG Dox (-)
tTA (-)
C
D
DAPI
Rheb
DAPI
Rheb
TnT
Merged
TnT
Merged

Fig. VI

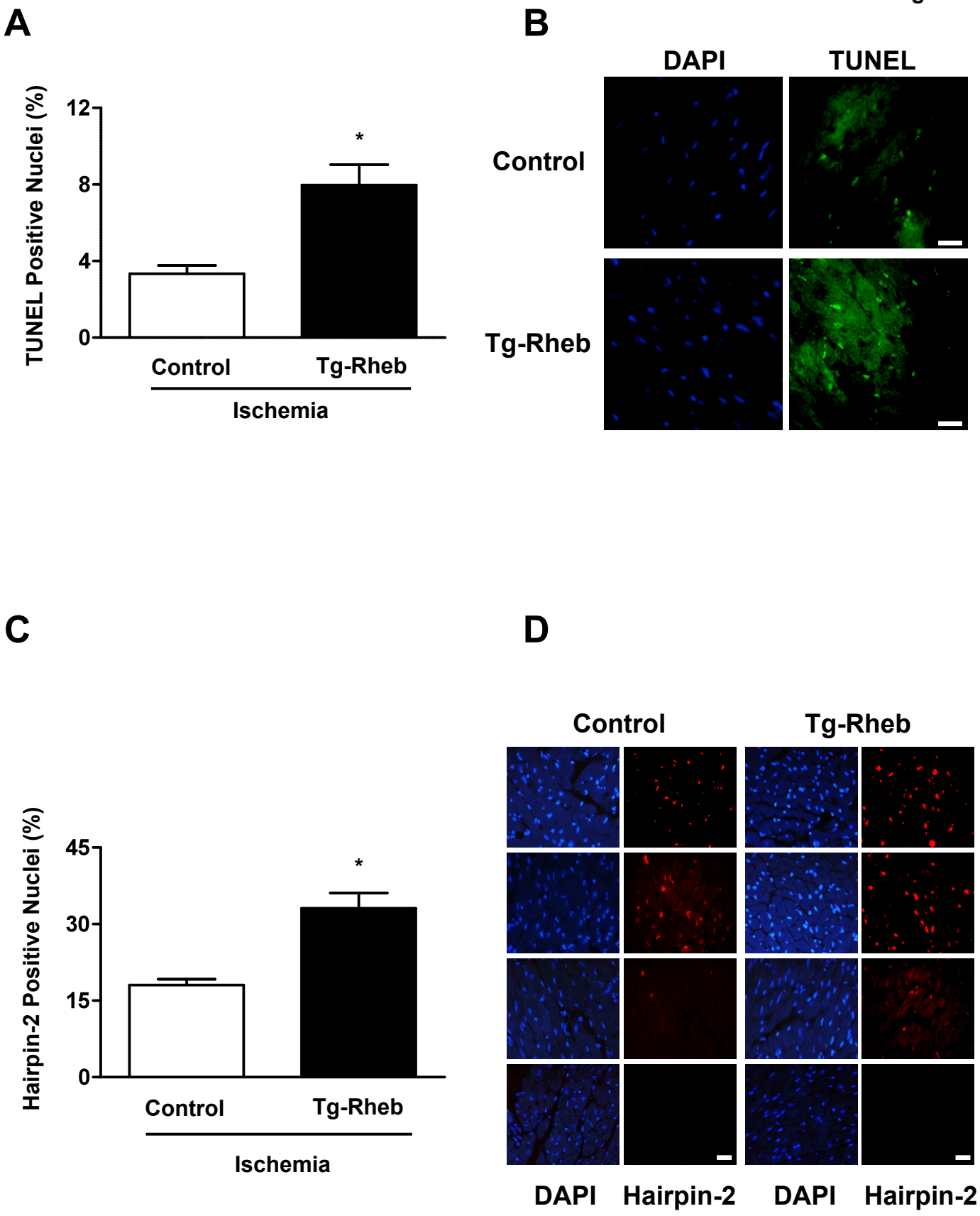
A
TUNEL Positive Nuclei (%)
12
8
4
0
*
Control
Tg-Rheb
Ischemia
B
DAPI
TUNEL
Control
Tg-Rheb
C
Hairpin-2 Positive Nuclei (%)
45
30
15
0
*
Control
Tg-Rheb
Ischemia
D
Control
Tg-Rheb
DAPI
Hairpin-2
DAPI
Hairpin-2

Fig. VII

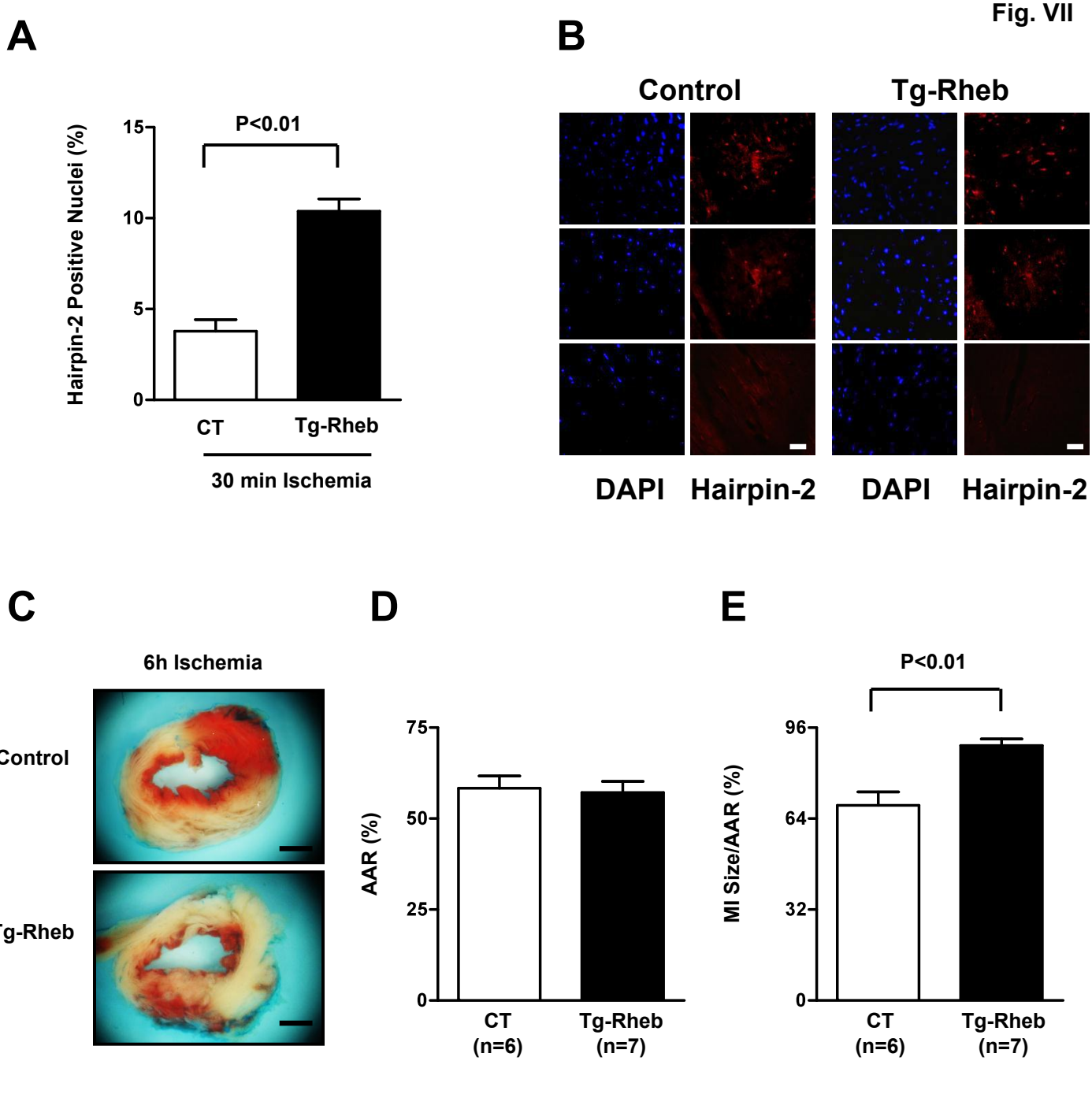
A
Hairpin-2 Positive Nuclei (%)
15
10
5
0
P<0.01
CT
Tg-Rheb
30 min Ischemia
B
Control
Tg-Rheb
DAPI
Hairpin-2
DAPI
Hairpin-2
C
6h Ischemia
Control
Tg-Rheb
D
AAR (%)
75
50
25
0
CT
(n=6)
Tg-Rheb
(n=7)
E
P<0.01
MI Size/AAR (%)
96
64
32
0
CT
(n=6)
Tg-Rheb
(n=7)

Fig. VIII

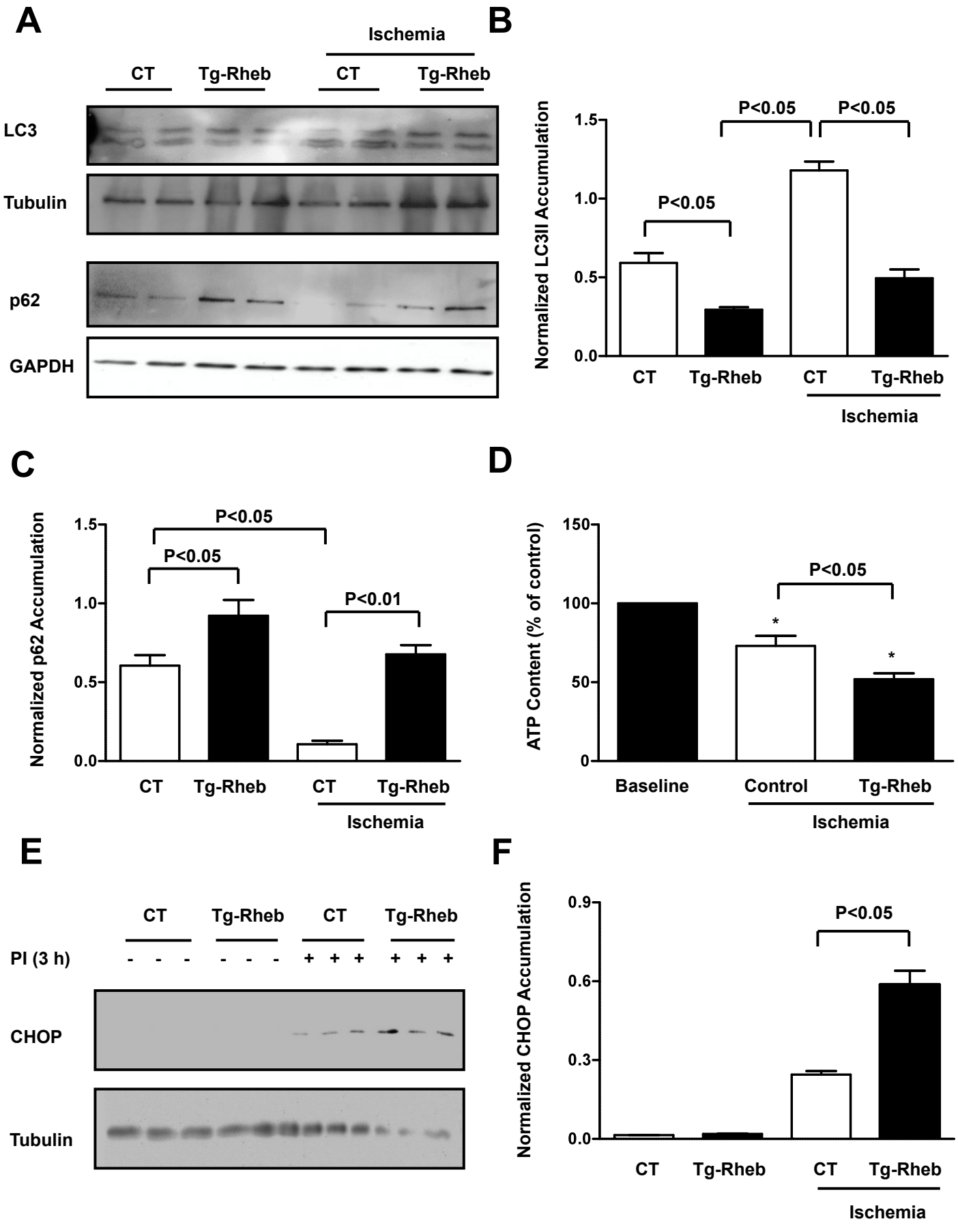
A
Ischemia
CT
Tg-Rheb
CT
Tg-Rheb
LC3
Tubulin
p62
GAPDH
B
Normalized LC3II Accumulation
P<0.05
P<0.05
P<0.05
1.5
1.0
0.5
0.0
CT
Tg-Rheb
CT
Tg-Rheb
Ischemia
C
Normalized p62 Accumulation
P<0.05
P<0.05
P<0.01
1.5
1.0
0.5
0.0
CT
Tg-Rheb
CT
Tg-Rheb
Ischemia
D
ATP Content (% of control)
P<0.05
150
100
50
0
*
*
Baseline
Control
Tg-Rheb
Ischemia
E
CT
Tg-Rheb
CT
Tg-Rheb
PI (3 h)
- - - - - - + + + + + +
CHOP
Tubulin
F
Normalized CHOP Accumulation
P<0.05
0.9
0.6
0.3
0.0
CT
Tg-Rheb
CT
Tg-Rheb
Ischemia

Fig. IX

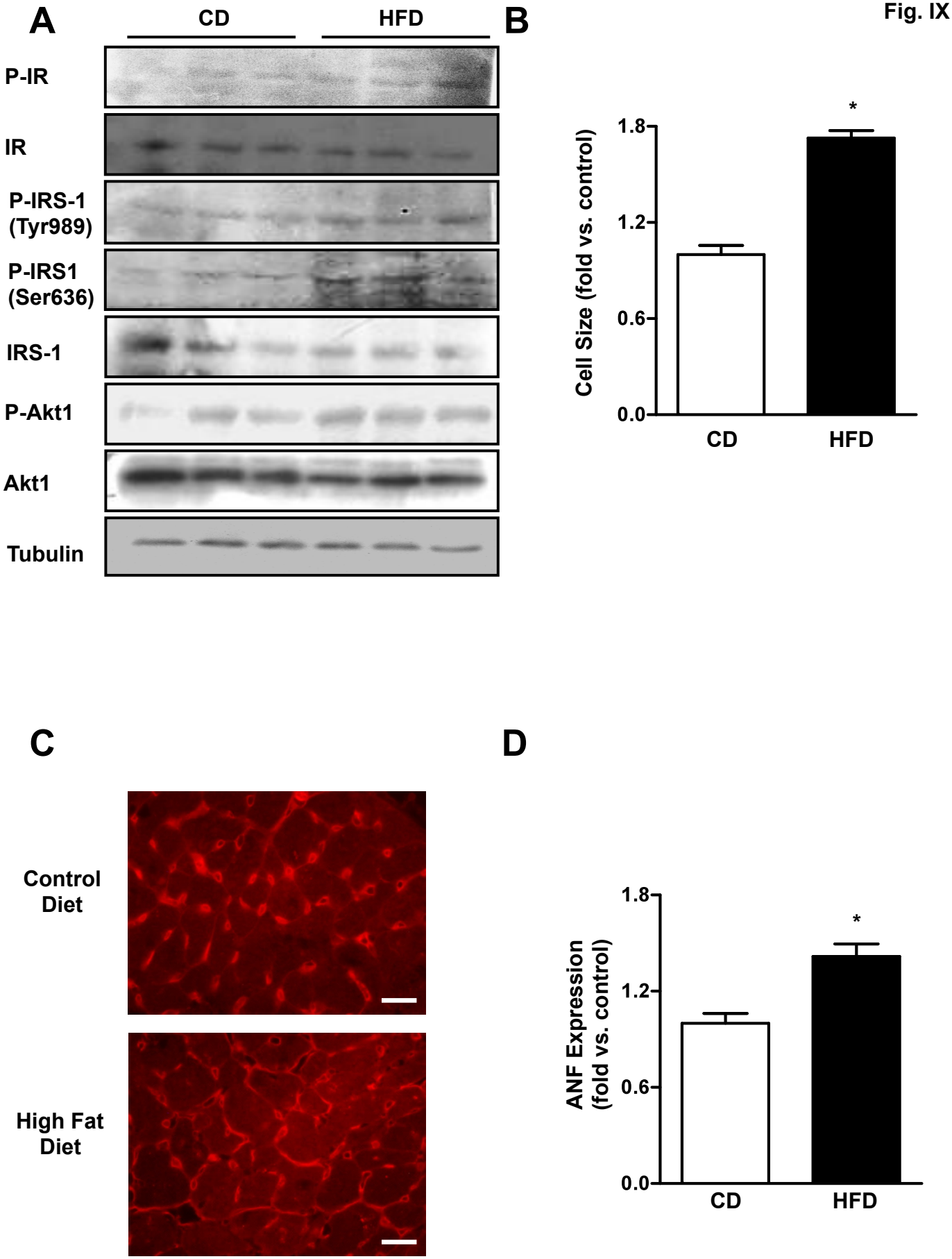
A
CD
HFD
P-IR
IR
P-IRS-1 (Tyr989)
P-IRS1 (Ser636)
IRS-1
P-Akt1
Akt1
Tubulin
B
Cell Size (fold vs. control)
1.8
1.2
0.6
0.0
*
CD
HFD
C
Control Diet
High Fat Diet
D
ANF Expression (fold vs. control)
1.8
1.2
0.6
0.0
*
CD
HFD

Fig. X

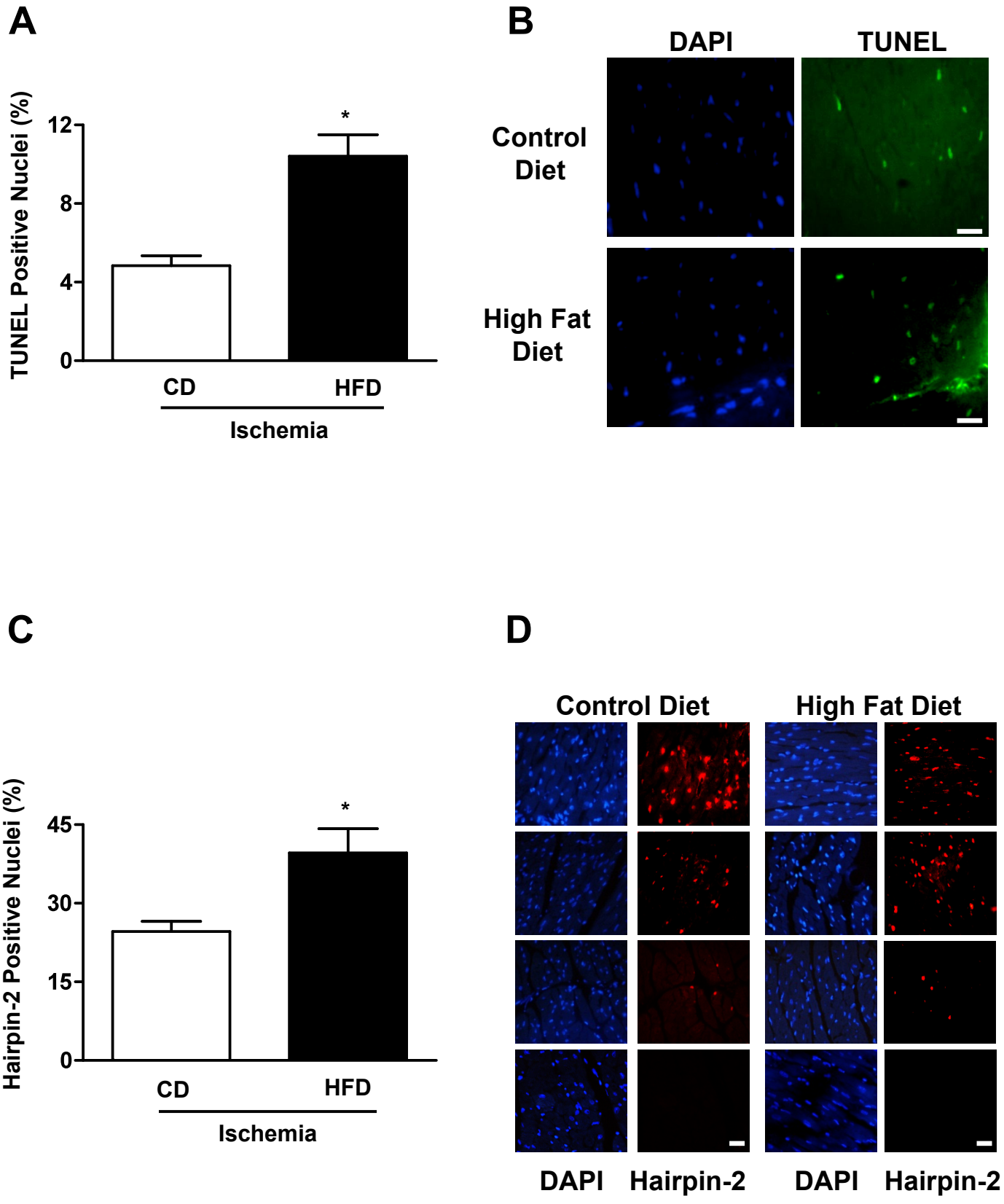
A
TUNEL Positive Nuclei (%)
12
8
4
0
*
CD
HFD
Ischemia
B
DAPI
TUNEL
Control Diet
High Fat Diet
C
Hairpin-2 Positive Nuclei (%)
45
30
15
0
*
CD
HFD
Ischemia
D
Control Diet
High Fat Diet
DAPI
Hairpin-2
DAPI
Hairpin-2

Fig. XI

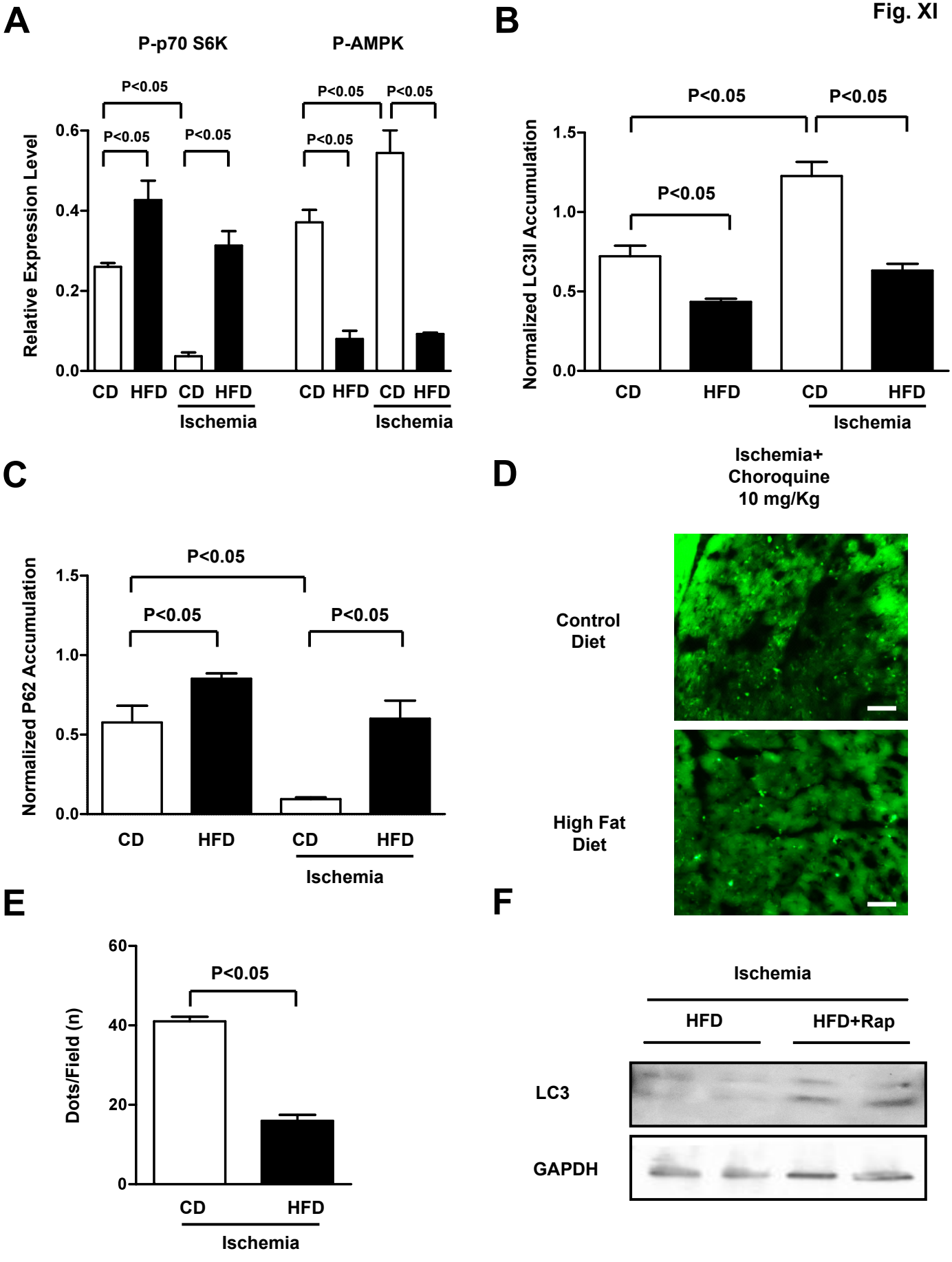
A
P-p70 S6K
P-AMPK
Relative Expression Level
P<0.05
0.6
0.4
0.2
0.0
CD HFD CD HFD
Ischemia
B
Normalized LC3II Accumulation
1.5
1.0
0.5
C
Normalized P62 Accumulation
D
Ischemia+
Choroquine
10 mg/Kg
Control
Diet
High Fat
Diet
E
Dots/Field (n)
60
40
20
0
F
HFD
HFD+Rap
LC3
GAPDH

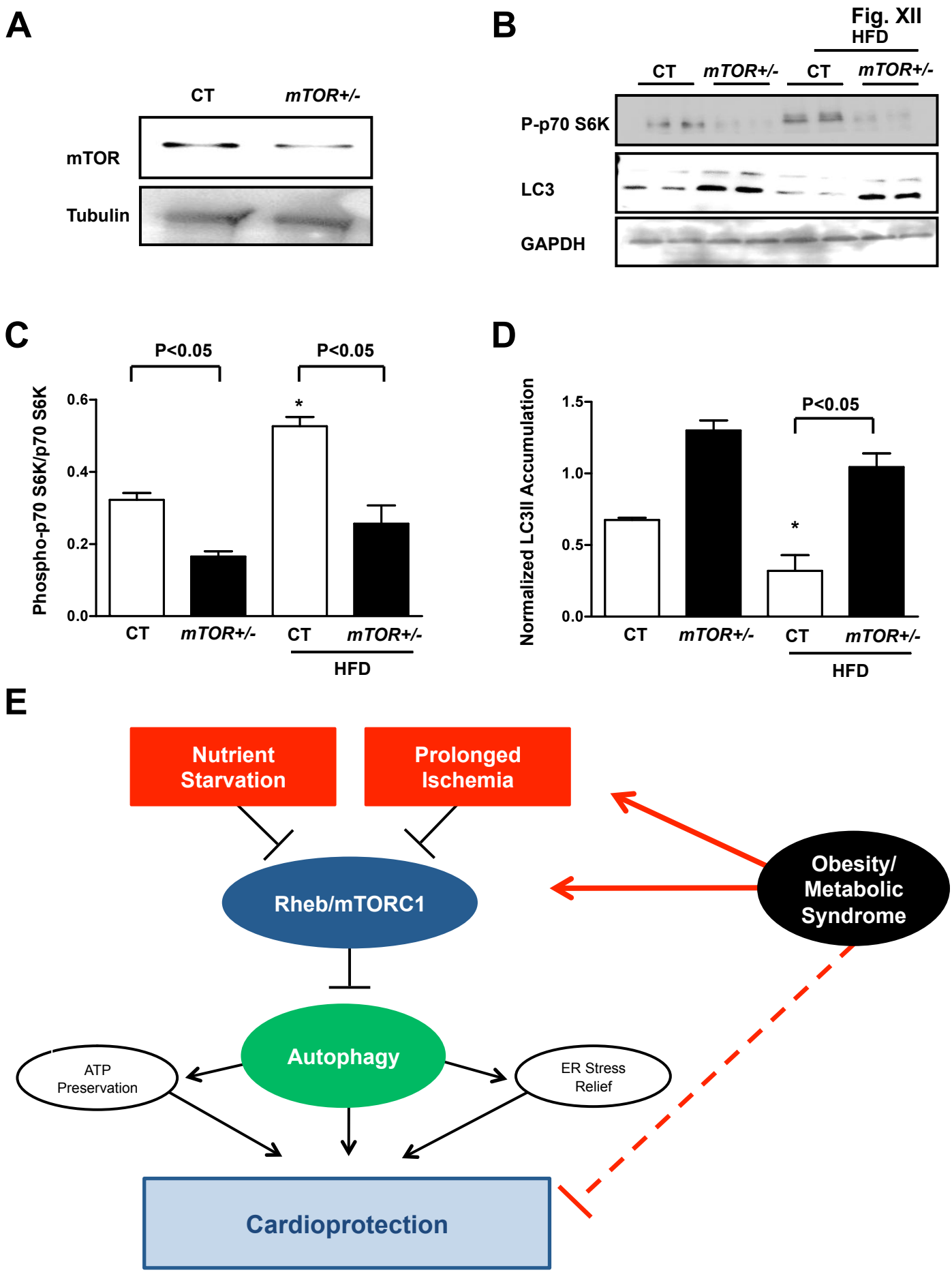
A
CT
mTOR+/-
mTOR
Tubulin
B
Fig. XII
HFD
CT
mTOR+/-
CT
mTOR+/-
P-p70 S6K
LC3
GAPDH
C
P<0.05
P<0.05
Phospho-p70 S6K/p70 S6K
0.6
0.4
0.2
0.0
*
CT
mTOR+/-
CT
mTOR+/-
HFD
D
Normalized LC3II Accumulation
1.5
1.0
0.5
0.0
P<0.05
*
CT
mTOR+/-
CT
mTOR+/-
HFD
E
Nutrient Starvation
Prolonged Ischemia
Rheb/mTORC1
Obesity/ Metabolic Syndrome
Autophagy
ATP Preservation
ER Stress Relief
Cardioprotection

Supplemental Figure Legends

Figure I. A, Rheb expression and phosphorylation status of $p70^{S6K}$ were evaluated in cardiomyocytes transduced with adenovirus expressing a short hairpin sequence, targeting Rheb for 96 hours. **B,** Phosphorylation status of $p70^{S6K}$ was evaluated in cardiomyocytes transduced with increasing doses of Ad-Rheb, after 4 hours of GD. **C,** Rheb was overexpressed in cardiomyocytes both at baseline and during GD, and it was then immunoprecipitated. Physical interaction between Rheb and mTOR was evaluated both at baseline and during glucose deprivation. **D-F,** Phosphorylation status of $p70^{S6K}$ was evaluated in cardiomyocytes with sh-TSC2 depletion, sh-Rheb, or with sh-TSC2 (D) and sh-Rheb together (E). Densitometric quantification is also shown. N=4 (F). **G-H,** mTORC2 activity, as assessed by the phosphorylation status of Akt (Ser 473), was evaluated in cardiomyocytes transduced with Ad-LacZ or Ad-Rheb, both at baseline and after 4 hours of GD. N=3.

Figure II. A, Cardiomyocytes were transduced with Ad-LacZ or Ad Rheb for 48 hours, or with sh-Rheb for 96 hours, and then subjected to GD for 18 hours. Percentage of propidium iodide-positive nuclei with respect to control cardiomyocytes was evaluated. N=3. **B,** Cardiomyocytes were transduced with sh-scramble or sh-TSC2 for 96 hours and then subjected to GD for 10 hours. TUNEL staining was performed. Data is presented as a percentage with respect to cells transduced with control adenovirus. Control bar is set at 100%. * $p<0.05$ vs. LacZ or Sh-CT. Bar=50 μm. N=3.

Figure III. A-C, Cardiomyocytes were transduced with sh-scramble, sh-TSC2 or sh-Rheb for 96 hours. LC3 isoforms and p62 accumulation were then evaluated at baseline or after 4 hours of GD. Representative immunoblots are shown (A), together with densitometric analyses of LC3-II (B) and p62 (C). N=4. **D-E,** Cardiomyocytes were coinfected with sh-scramble or sh-TSC2 for 96 hours and adenovirus expressing GFP-LC3 for the last 48 hours. After 4 hours of GD, GFP-LC3 puncta were counted. The percentage of cardiomyocytes with GFP-LC3 dots among those transduced with sh-scramble or sh-TSC2 is shown (D, * $p<0.05$), together with representative images. N=5 (E, bar=10

μm). **F-G,** Cardiomyocytes were coinfected with sh-scramble or sh-Rheb for 96 hours and adenovirus expressing GFP-LC3 for the last 48 hours. The baseline percentage of cardiomyocytes with GFP-LC3 dots among those transduced with sh-scramble or sh-Rheb is shown (F, * $p<0.05$; N=4), together with representative images (G, bar=10 μm).

Figure IV. A, Atg7 expression levels were evaluated in cardiomyocytes transduced with Ad-LacZ or Ad-Atg7. **B,** LC3-II and p62 expression levels were evaluated in cardiomyocytes transduced with Ad-LacZ, Ad-Rheb, or with Ad-Rheb together with Ad-Atg7. **C-D,** Cardiomyocytes were infected with Ad-GFP-LC3 together with Ad-LacZ or Ad-Rheb or Ad-Rheb and Ad-Atg7 together. Percentage of cardiomyocytes with GFP-LC3 puncta was evaluated during GD; bar=10 μm. N=3. **E-F,** Expression levels of LC3-II, p62, phospho-$p70^{s6k}$, Atg7 and Beclin-1 were evaluated in Ad-LacZ- and Ad-Rheb-transduced cardiomyocytes treated, or not treated, with trehalose.

Figure V. A-B, Normalized cardiac Rheb expression was evaluated in double transgenic mice ($Rheb^+$ and tTA^+; DTG) not treated with doxycycline, in DTG mice treated with doxycycline, and in $Rheb^+/tTA^-$ mice. Representative immunoblot is presented (A) with expression levels quantified (B). N=3; * $p<0.05$ vs. Dox(+) and tTA (-). **C-D,** LV myocardial tissue sections from control mice and Tg-Rheb were stained with Rheb antibody (green fluorescence) and troponin T (red fluorescence), and then counterstained with DAPI (blue fluorescence) for nuclei visualization. Representative separate and merged panels from control (C) and Tg-Rheb (D) are presented. Bar= 50 μm.

Figure VI. A-B, LV myocardial sections of Tg-Rheb and controls were subjected to TUNEL and DAPI staining. The percentage of cells that were TUNEL positive is shown. * $p<0.05$; N=3. Representative images of the staining in the border zone are shown (B, bar=50 μm). **C-D,** Tg-Rheb presented a higher necrosis rate after ischemia. LV myocardial sections were subjected to hairpin-2 and DAPI staining. The percentage of cells that were hairpin-2 positive is shown. * $p<0.05$; N=3 (C).

Representative images of the staining in the ischemic and non-ischemic areas are shown (D, bar=50 μm).

Figure VII. A-B, Tg-Rheb and control mice were subjected to 30 minutes of ischemia. The extent of myocardial necrosis was evaluated with Hapirpin 2 staining. The quantitative analysis of Hairpin 2 staining is shown in A. Representative Hairpin 2 staining is shown in B N=4. **C-E,** Tg-Rheb and control mice were subjected to 6 hours of ischemia. Representative images of the TTC staining/alcian blue staining is shown in C. Bar=50 μm. The quantitative analysis of AAR and MI size/AAR is shown in D and E, respectively.

Figure VIII. A-C, Autophagy was evaluated in Tg-Rheb at baseline and after 30 minutes or 3 hours of ischemia, as assessed by LC3-II and p62 accumulation, respectively. A representative immunoblot is presented (A), together with the densitometric analyses of LC3 (B) and p62 (C). N=4 for each group. **D,** ATP content was assessed in the ischemic area of the left ventricles after 3 hours of ischemia. Data is presented as the percentages of respective baselines. Baseline is represented as one bar arbitrarily set at 100%. * $p<0.05$ with respect to relevant baseline. N=5. **E-F,** Cardiac CHOP expression was evaluated in Tg-Rheb and controls at baseline and after 3 hours of ischemia. A representative blot is shown (E), together with the densitometric analysis; N=5 for each group (F).

Figure IX. A, Phosphorylation status of insulin receptor β (Tyr1162/3), phosphorylation of insulin receptor substrate-1 (Tyr989, Ser 636), and phosphorylation of Akt1 (Ser473) were evaluated in HFD mice and compared to control animals. **B-C,** Cell size was evaluated through WGA staining in the heart of HFD mice with respect to controls. Cell size quantification is presented as fold vs. control, which is set at 1. * $p<0.05$. In C, Representative images are also presented. N=4. Bar=50 μm. **D,** ANF expression resulted to be increased in HFD mice with respect to controls. Data is presented as fold vs. CD mice. * $p<0.05$. N=6.

Figure X. A-B, HFD mice presented a higher apoptosis rate in the ischemic area after ischemia. LV myocardial sections were subjected to TUNEL and DAPI staining. The percentage of cells that were TUNEL-positive is shown. * $p<0.05$; N=3 (A). In B, representative images of the staining in the border zone are shown. Bar=50 μm. **C-D,** HFD mice presented a higher necrosis rate after ischemia. LV myocardial sections were subjected to hairpin-2 and DAPI staining. The percentage of cells that were hairpin-2 positive is presented. * $p<0.05$; N=3. In D, Representative images of the staining in the ischemic and non-ischemic areas are shown. Bar=50 μm.

Figure XI. A, HFD mice present an increase in phosphorylation status of $p70^{S6K}$ and AMPK in the heart. Representative immunoblots are presented in Fig. 7D. N=4 for each group. **B-C,** Myocardial autophagy in obese mice was significantly inhibited compared to that in lean mice, both at baseline and after 30 minutes or 3 hours of ischemia, as indicated by LC3-II and p62 accumulation, respectively. N=4 for each group. Representative immunoblots are presented in Figure 7F. **D-E,** Chloroquine (10 mg/kg) was administered to Tg-GFP-LC3 mice fed with control diet or HFD, 4 hours before surgery. After 30 minutes of ischemia, GFP-LC3 puncta were counted in LV sections. In D, representative images are presented. Bar=50 μm. In E, quantification of the number of dots/field is shown. N=3. **F,** Rapamycin (1 mg/kg) was administered intraperitoneally to HFD and CD mice 60 minutes before coronary ligation. After 30 minutes of ischemia, autophagy was evaluated by LC3-II accumulation in the hearts of HFD mice treated with rapamycin, with respect to HFD mice treated with vehicle.

Figure XII. A, Tamoxifen (30 μg/g) was administered to α-MHC-*MerCreMer-mTOR flox/+* mice (*mTOR*+/-) and α-MHC-*MerCreMer-mTOR* +/+ mice (controls) for 7 days. Cardiac mTOR protein levels were evaluated in *mTOR*+/- and controls 3 weeks after tamoxifen administration. **B-D,** Cardiac phosphorylation status of $p70^{S6K}$, and LC3-II accumulation were evaluated in *mTOR*+/- mice and controls, fed with control diet or HFD (N=4). * $p<0.05$ vs. CT. **E,** A schematic representation of our hypothesis. Nutrient starvation and prolonged ischemia inhibit the mTORC1 pathway through Rheb

inhibition. Rheb/mTORC1 inhibition upregulates autophagy, which increases cardioprotection. On the other hand, obesity and metabolic syndrome activate the Rheb/mTORC1 pathway during prolonged ischemia, causing a defective activation of autophagy and a reduction in cardioprotection.

Supplemental References

1. Sanbe A, Gulick J, Hanks MC, Liang Q, Osinska H, Robbins J. Reengineering inducible cardiac-specific transgenesis with an attenuated myosin heavy chain promoter. *Circ Res.* 2003;92:609-616.

2. Matsui Y, Nakano N, Shao D, Gao S, Luo W, Hong C, Zhai P, Holle E, Yu X, Yabuta N, Tao W, Wagner T, Nojima H, Sadoshima J. Lats2 is a negative regulator of myocyte size in the heart. *Circ Res.* 2008;103:1309-1318.

3. Vivaldi MT, Kloner RA, Schoen FJ. Triphenyltetrazolium staining of irreversible ischemic injury following coronary artery occlusion in rats. *Am J Pathol.* 1985;121:522-530.

4. Hsu CP, Oka S, Shao D, Hariharan N, Sadoshima J. Nicotinamide phosphoribosyltransferase regulates cell survival through NAD+ synthesis in cardiac myocytes. *Circ Res.* 2009;105:481-491.

5. Didenko VV, Ngo H, Baskin DS. Early necrotic DNA degradation: presence of blunt-ended DNA breaks, 3' and 5' overhangs in apoptosis, but only 5' overhangs in early necrosis. *Am J Pathol.* 2003;162:1571-1578.

6. Guerra S, Leri A, Wang X, Finato N, Di Loreto C, Beltrami CA, Kajstura J, Anversa P. Myocyte death in the failing human heart is gender dependent. *Circ Res.* 1999;85:856-866.

7. Usui S, Maejima Y, Pain J, Hong C, Cho J, Park JY, Zablocki D, Tian B, Glass DJ, Sadoshima J. Endogenous muscle atrophy F-box mediates pressure overload-induced cardiac hypertrophy through regulation of nuclear factor-kappaB. *Circ Res.* 2011;109:161-171.

8. Matsui Y, Takagi H, Qu X, Abdellatif M, Sakoda H, Asano T, Levine B, Sadoshima J. Distinct roles of autophagy in the heart during ischemia and reperfusion: roles of AMP-activated protein kinase and Beclin 1 in mediating autophagy. *Circ Res.* 2007;100:914-922.

9. Mizushima N, Yoshimori T, Levine B. Methods in mammalian autophagy research. *Cell.* 2010;140:313-326.

10. Perry CN, Kyoi S, Hariharan N, Takagi H, Sadoshima J, Gottlieb RA. Novel methods for measuring cardiac autophagy in vivo. *Methods Enzymol.* 2009;453:325-342.

11. Inoki K, Li Y, Xu T, Guan KL. Rheb GTPase is a direct target of TSC2 GAP activity and regulates mTOR signaling. *Genes Dev.* 2003;17:1829-1834.

12. Karbowniczek M, Cash T, Cheung M, Robertson GP, Astrinidis A, Henske EP. Regulation of B-Raf kinase activity by tuberin and Rheb is mammalian target of rapamycin (mTOR)-independent. *J Biol Chem.* 2004;279:29930-29937.

13. Im E, von Lintig FC, Chen J, Zhuang S, Qui W, Chowdhury S, Worley PF, Boss GR, Pilz RB. Rheb is in a high activation state and inhibits B-Raf kinase in mammalian cells. *Oncogene.* 2002;21:6356-6365.

14. Sharma PM, Egawa K, Huang Y, Martin JL, Huvar I, Boss GR, Olefsky JM. Inhibition of phosphatidylinositol 3-kinase activity by adenovirus-mediated gene transfer and its effect on insulin action. *J Biol Chem.* 1998;273:18528-18537.

15. Scheele JS, Rhee JM, Boss GR. Determination of absolute amounts of GDP and GTP bound to Ras in mammalian cells: comparison of parental and Ras-overproducing NIH 3T3 fibroblasts. *Proc Natl Acad Sci U S A.* 1995;92:1097-1100.